Thermodynamic and Kinetic Characterization of Co−C Bond Homolysis Catalyzed by Coenzyme B_{12}-Dependent Methylmalonyl-CoA Mutase†

Shantanu Chowdhury and Ruma Banerjee*

Biochemistry Department, University of Nebraska, Lincoln, Nebraska 68588-0664

Received November 3, 1999; Revised Manuscript Received April 20, 2000

ABSTRACT: Methylmalonyl-CoA mutase is a member of the family of coenzyme B_{12}-dependent isomerases and catalyzes the 1,2-rearrangement of methylmalonyl-CoA to succinyl-CoA. A common first step in the reactions catalyzed by coenzyme B_{12}-dependent enzymes is cleavage of the cobalt−carbon bond of the cofactor, leading to radical-based rearrangement reactions. Comparison of the homolysis rate for the free and enzyme-bound cofactors reveals an enormous rate enhancement which is on the order of a trillion-fold. To address how this large rate acceleration is achieved, we have examined the kinetic and thermodynamic parameters associated with the homolysis reaction catalyzed by methylmalonyl-CoA mutase. Both the rate and the amount of cob(II)alamin formation have been analyzed as a function of temperature with the protiated substrate. These studies yield the following activation parameters for the homolytic reaction at 37 °C: $\Delta H_f^{\ddagger} = 18.8 \pm 0.8$ kcal/mol, $\Delta S_f^{\ddagger} = 18.2 \pm 0.8$ cal/(mol·K), and $\Delta G_f^{\ddagger} = 13.1 \pm 0.6$ kcal/mol. Our results reveal that the enzyme lowers the transition state barrier by 17 kcal/mol, corresponding to a rate acceleration of 0.9×10^{12}-fold. Both entropic and enthalpic factors contribute to the observed rate acceleration, with the latter predominating. The substrate binding step is exothermic, with a ΔG of −5.2 kcal/mol at 37 °C, and is favored by both entropic and enthalpic factors. We have employed the available kinetic and spectroscopic data to construct a qualitative free energy profile for the methylmalonyl-CoA mutase-catalyzed reaction.

Coenzyme B_{12}- (or AdoCbl-)[1] dependent enzymes achieve spectacular rate enhancements in the homolytic cleavage of the organometallic Co−C bond that initiates their radical-based isomerization reactions. Members of this family of enzymes catalyze 1,2-rearrangement reactions in which the migrating group and a hydrogen atom on vicinal carbons interchange positions. Methylmalonyl-CoA mutase is the only member of this group of enzymes that is found in both bacterial and animal kingdoms and catalyzes the rearrangement of methylmalonyl-CoA to succinyl-CoA (*1*, *2*). The first step in all these reactions is postulated to be homolysis of the Co−C bond of the cofactor, generating a pair of radicals. In methylmalonyl-CoA mutase (Scheme 1), glutamate mutase, and ribonucleotide reductase, there is strong kinetic evidence that the Co−C bond cleavage step is kinetically coupled to formation of the next radical in the reaction pathway. For methylmalonyl-CoA mutase (*3*) and glutamate mutase (*4*), this represents a carbon-centered substrate radical, whereas in ribonucleotide reductase this corresponds to a protein-based thiyl radical (*5*).

The bond dissociation enthalpy for the Co−C bond in base-on AdoCbl in solution is 30 ± 2 kcal/mol (*6*, *7*) and the homolysis rate constant for the uncatalyzed reaction is 3.8×10^{-9} s^{-1} at 37 °C (calculated from the $\Delta H^{\ddagger}_{hom}$ and $\Delta S^{\ddagger}_{hom}$ values in ref *7*). In the various AdoCbl-dependent enzymes, the k_{cat} for the reaction is of the order of $\sim 10^2$ s^{-1}. Thus, the enzymes orchestrate an approximately 10^{11}-fold rate acceleration for the homolysis of the Co−C bond (*8*). The strategy employed by the isomerases to labilize the Co−C bond has been the subject of intense debate, with models for destablization by conformational distortion of the corrin ring (*9*−*13*) and electronic trans effects (*14*, *15*) having been extensively explored. Comparison of the Co−C stretching vibration frequency of free and methylmalonyl-CoA mutase-bound cofactor by resonance Raman spectroscopy have indicated minimal ground-state destabilization of the Co−C bond (*16*−*19*). Thus, from the minor frequency downshift observed for the bound versus the free cofactor it was estimated that the Co−C bond is ∼0.5 kcal/mol weaker in the mutase active site (*18*). These data indicate that the predominant labilization of the Co−C bond occurs following binding of substrate.

In this study, we have determined the thermodynamic parameters associated with Co−C bond cleavage in the methylmalonyl-CoA mutase-catalyzed reaction using stopped-flow UV−visible spectroscopy. A minimal scheme describing the mutase-catalyzed reaction is presented in Scheme 1. According to this mechanism, binding of substrate to holoenzyme leads to the formation of a Michaelis−Menten complex. The subsequent homolytic cleavage of the Co−C bond (k_1) is accompanied by a change in the UV−visible spectrum as AdoCbl is converted to cob(II)alamin. Kinetic evidence supports coupling of the homolysis step (k_1) to

† This work was supported by a grant from the National Institutes of Health (DK45776). R.B. is an Established Investigator of the American Heart Association.

* Corresponding author: tel 402-472-2941; fax 402-472-7842; e-mail rbanerjee1@unl.edu.

[1] Abbreviations: AdoCbl, 5′-deoxyadenosylcobalamin or coenzyme B_{12}; Co−C bond, cobalt−carbon bond; CoA, coenzyme A; dAdo, deoxyadenosine.

10.1021/bi992535e CCC: $19.00
Published on Web 06/14/2000

Scheme 1

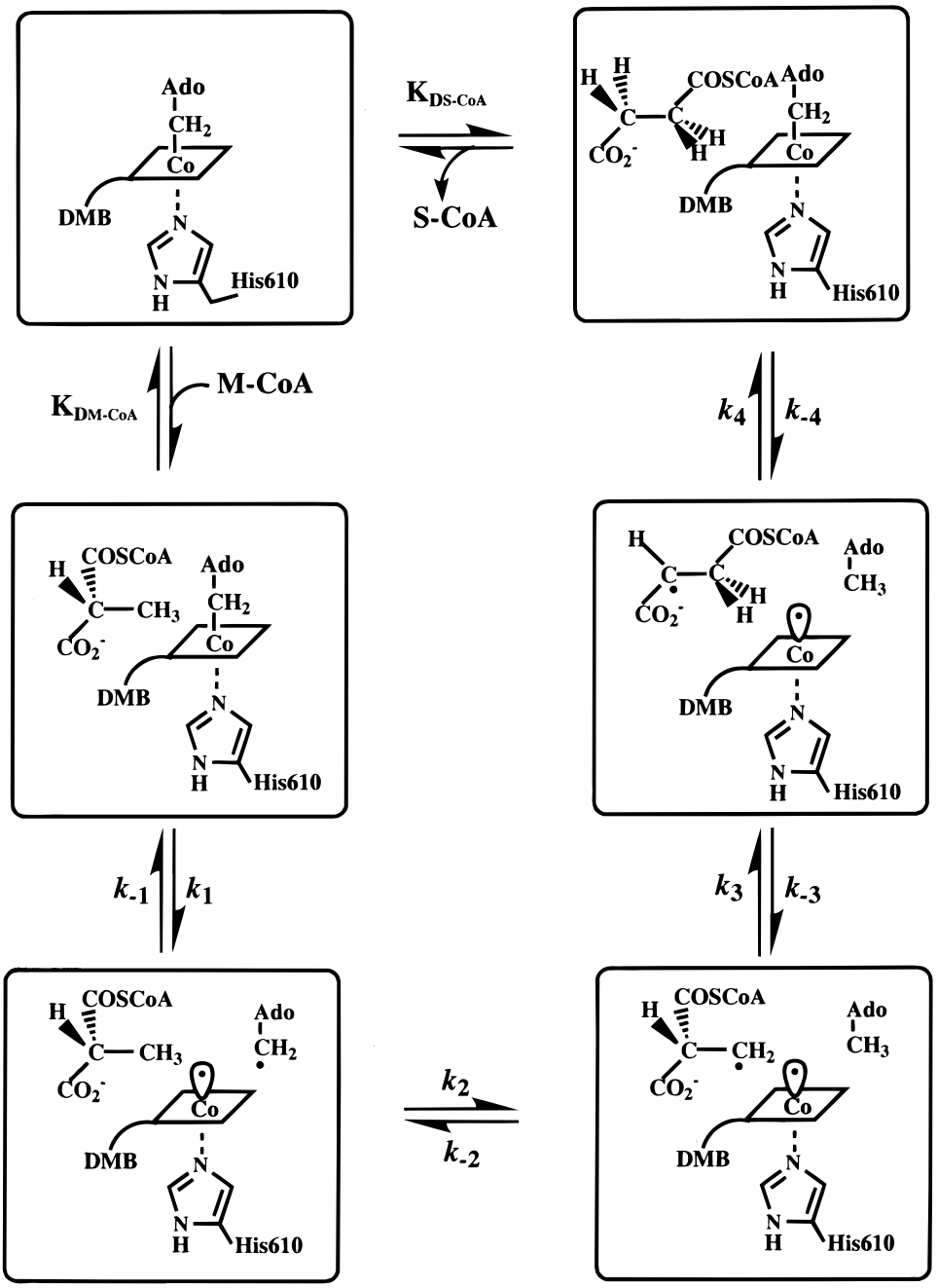

hydrogen atom abstraction (k_2) (*3*). Isomerization (k_3) and radical recombination (k_4) steps lead to product and to the reformation of AdoCbl. Analysis of the temperature dependence of the substrate binding and cob(II)alamin formation steps provide the respective thermodynamic parameters. Our results reveal that substrate binding is exothermic and the activation parameters for the Co−C bond homolysis step are significantly altered compared to the uncatalyzed reaction. Both enthalpic and entropic factors contribute to lowering of the activation energy for Co−C bond homolysis with the former predominating.

MATERIALS AND METHODS

Materials. Protocatechuic acid, AdoCbl, and (*R*,*S*)-[CH_3]-methylmalonyl-CoA were purchased from Sigma. Protocatechuate dioxygenase was a gift from John Lipscomb (University of Minnesota). Radioactive [$^{14}CH_3$]methylmalonyl-CoA (56.4 Ci/mol) was purchased from New England Nuclear. All other chemicals were reagent-grade commercial products and were used without further purification.

Enzyme Expression and Purification. The recombinant expression vector (pMEX2/pGP1−2) harboring the *Propionibacterium shermanii* genes in *Escherichia coli* strain K 38 (*20*) was a gift from Peter Leadlay (Cambridge University). The enzyme was purified, reconstituted with AdoCbl, and separated from unbound cofactor by FPLC as described before (*21*).

Enzyme Assays. Enzyme activity of the mutase was determined in the radiolabeled assay at 37 °C as described previously (*22*) and was 29 units/mg of protein. One unit of activity catalyzes the formation of 1 μmol of succinyl-CoA/min at 37 °C.

Stopped-Flow UV−Visible Spectroscopy. Pre-steady-state kinetic experiments were carried out in an Olis stopped-flow UV−vis spectrophotometer. An external water bath was used to maintain the loading syringes and the mixing chamber at the desired temperature (±0.5 °C). The syringes, tubing, and mixing chamber of the stopped-flow apparatus were deoxygenated by filling the drive syringes with a solution containing 400 μM protocatechuic acid and 0.2 unit of protocatechuate dioxygenase in 50 mM potassium phosphate buffer (pH 7.5) for at least 3 h before initiation of the experiments. The solution of holomethylmalonyl-CoA mutase (30 or 40 μM in bound AdoCbl before mixing) in anaerobic 50 mM potassium phosphate buffer, pH 7.5, was transferred to a tonometer inside a Coy anaerobic chamber. An anaerobic solution of (*R,S*)-[CH_3]-methylmalonyl-CoA (0.30−60 mM before mixing) in 50 mM potassium phosphate buffer, pH 7.5, was also transferred to a tonometer inside the anaerobic chamber. The methylmalonyl-CoA mutase and [CH_3]-methylmalonyl-CoA solutions were quickly transferred from the tonometer to the deoxygenated loading syringes, and the solutions were allowed to equilibrate for at least 15 min before initiation of the experiments. The concentration of holomethylmalonyl-CoA mutase was determined spectrophotometrically (ϵ_{525} = 8000 M^{-1} cm^{-1}). Formation of cob(II)alamin was monitored by a decrease in absorption at 525 nm. For conversion of AdoCbl to cob(II)alamin, $\Delta\epsilon_{525nm}$ = 4800 M^{-1} cm^{-1} was used (*23*). Analysis of the kinetic traces was performed with SigmaPlot (Jandel Scientific). Experiments with holomethylmalonyl-CoA mutase were performed under reduced illumination.

Substrate Dependence of Co−C Bond Homolysis Rate at Different Temperatures. Holomethylmalonyl-CoA mutase (30 or 40 μM) in 50 mM potassium phosphate buffer, pH 7.5, was mixed with an equal volume of the same reaction buffer containing variable amounts of (*R, S*)-methylmalonyl-CoA (0.30−60 mM) and the change in absorbance was monitored at 525 nm. To approximate pseudo-first-order conditions, the concentration of (*R*)-methylmalonyl-CoA was in 5−750-fold excess of enzyme after mixing (the concentration of the *R*-isomer is estimated on the basis of the assumption that the *R* and *S* isomers are present in a 1:1 mixture). Thus, the concentration of methylmalonyl-CoA mutase was 15 μM (after mixing) when 75 μM substrate was employed; for all other substrate concentrations it was 20 μM (after mixing). Experiments were carried out at 5, 10, 12, 15, 18, and 20 °C at each set of protiated substrate concentrations. Kinetic traces were fit to a single-exponential function by use of SigmaPlot (Jandel Scientific) to obtain k_{obs} and the change in amplitude, ΔA, according to eq 1, where A_t is the absorbance at time t and A_i is the offset for the exponential decay. All experiments were run at least in duplicate.

$$A_t = A_i + \Delta A \exp(-k_{obs}t) \quad (1)$$

Estimation of Thermodynamic Activation Parameters from the Temperature Dependence of k_{obs} as a Function of Substrate Concentration. The values for k_{obs} determined between 5 and 20 °C were plotted as a function of temperature by use of the Arrhenius equation at each substrate concentration (Figure 1, inset). The best-fit values for k_{obs} ($r^2 \sim 0.999$) were used subsequently instead of individual k_{obs} values to avoid random errors in the determination of k_{obs} (*24*). These values for k_{obs} were used in Figure 2, which displays the dependence of k_{obs} on substrate concentration at six different temperatures. Nonlinear least-squares fits of the plots in Figure 2 to eq 2 yield values for the parameters K_d, k_f, and k_r:

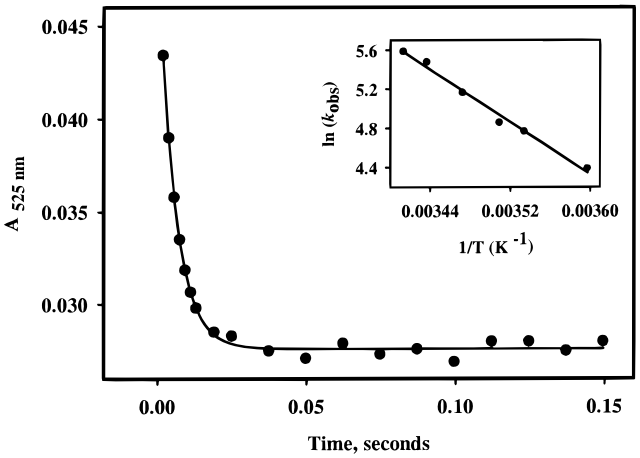

FIGURE 1: Representative kinetic trace for homolysis of enzyme-bound AdoCbl in the presence of substrate. A decrease in absorbance at 525 nm with time is observed after substrate (*R*)-[CH_3]-methylmalonyl-CoA (1.5 mM after mixing) is mixed with holomethylmalonyl-CoA mutase (20 μM after mixing) at 20 °C. k_{obs} was obtained by fitting the trace to eq 1. (Inset) Representative Arrhenius plot showing the temperature dependence of k_{obs} at 1.5 mM (*R*)-[CH_3]-methylmalonyl-CoA and 20 μM methylmalonyl-CoA mutase. A linear least-squares fit (r^2 = 0.999) was generated to obtain k_{obs} at different temperatures for each substrate concentration. Similar plots were generated for each substrate concentration.

$$k_{obs} = (k_f[S]/(K_d + [S])) + k_r \quad (2)$$

k_f is the rate constant for all steps leading to the formation of cob(II)alamin (k_1, k_2, and possibly k_3 in Scheme 1), k_r is the rate constant for all steps leading to the re-formation of AdoCbl from cob(II)alamin, and [S] represents the initial concentration of (*R*)-methylmalonyl-CoA. It should be noted that k_f is a complex macroscopic rate constant since only the formation of cob(II)alamin is being monitored and distinction between the Ado$^\bullet$, S$^\bullet$, and P$^\bullet$ radicals, each of which can exist in the presence of cob(II)alamin, is not possible in these experiments. Equation 2 is applicable to large perturbations from equilibrium observed with relaxation methods under pseudo-first-order conditions. The rate constant for approach to equilibrium for the homolysis step is linked to a bimolecular association step, i.e., substrate binding (Scheme 1). Hence, the rate of cob(II)alamin formation is predicted by eq 2 to follow saturation kinetics; that is, at high substrate concentration, when [S] $\gg K_d$, $k_{obs} = k_f + k_r$. Contribution from the reverse reaction, i.e., conversion of succinyl-CoA to methylmalonyl-CoA, is assumed to be negligible, since the product concentration is very low in the time scale of these experiments. The estimated value of K_d was used to obtain K_1 ($1/K_d$) at each temperature (Table 1). Thermodynamic activation parameters for the Co−C homolysis step were evaluated in an Eyring plot (Figure 3) according to

$$\ln (k/T) = \ln (k_B/h) - \Delta H_f^{\ddagger}/RT + \Delta S_f^{\ddagger}/R \quad (3)$$

In this equation, k is the rate constant, R is the universal gas

Table 1: Summary of Rate and Equilibrium Constants Obtained from Fits of k_{obs} to Eq 2

temp. (°C)	K_d (μM)	K_1[a] (M^{-1})	k_f (s^{-1})	k_r (s^{-1})
5	99 ± 35	10152 ± 3607	33 ± 5	48 ± 6
10	105 ± 23	9523 ± 2085	68 ± 7	50 ± 7
12	111 ± 1	9009 ± 892	76 ± 3	54 ± 4
15	114 ± 17	8771 ± 1308	121 ± 8	58 ± 8
18	118 ± 9	8474 ± 610	183 ± 6	60 ± 6
20	120 ± 7	8333 ± 506	208 ± 5	62 ± 6

[a] K_1 is $1/K_d$.

Table 2: Temperature Dependence of K_1 Obtained from Fits of ν to Eq 5

temp (°C)	K_d (μM)	K_1[a] (M^{-1})
5	98 ± 29	10193 ± 3013
10	107 ± 22	9345 ± 1921
12	112 ± 23	8928 ± 1833
15	116 ± 5	8620 ± 371
18	120 ± 13	8333 ± 903
20	125 ± 15	8000 ± 960

[a] K_1 is $1/K_d$.

constant, T is the temperature, k_B is the Boltzmann constant, h is Planck's constant, $\Delta H_f^{\ddagger}$ is the enthalpy of activation, and $\Delta S_f^{\ddagger}$ is the entropy of activation. The temperature dependence of the equilibrium constant K_1 was analyzed according to the van't Hoff equation to determine the thermodynamic parameters associated with the substrate binding step (Figure 4):

$$\ln (K_1) = -\Delta H_1/RT + \Delta S_1/R \quad (4)$$

For analysis of thermodynamic parameters associated with K_1, a standard state of 1 M was used.

Estimation of Thermodynamic Activation Parameters from the Temperature Dependence of [Cob(II)alamin]$_\infty$/[Mutase]$_0$ Concentration as a Function of Methylmalonyl-CoA Concentration. In a similar analysis, the fraction of enzyme present in the cob(II)alamin form (ν) at steady state was analyzed as a function of methylmalonyl-CoA concentration (Figure 5) to derive the equilibrium constant K_d, (*24*):

$$\nu = K_2'[S]/(K_d + [S] + K_2'[S]) \quad (5)$$

Here [S] is the initial substrate concentration and the equilibrium constant K_2' represents all the equilibrium steps following formation of the Michaelis complex. The estimated values for ν were plotted as ln ν versus $1/T$ for each substrate concentration. The linear functions that gave the best fits to these plots were used to interpolate values for ν at a given temperature and substrate concentration (not shown). Values of ν obtained in this way are statistically corrected for random errors and were plotted against methylmalonyl-CoA concentration and nonlinear least-squares fit to eq 5 yielded K_d and K_2' (Figure 5). The temperature dependence of $1/K_d$ between 5 and 20 °C was plotted in a van't Hoff plot, and eq 4 was used to obtain the thermodynamic parameters (Table 2).

RESULTS

Binding of substrate to holoenzyme is followed by cleavage of the Co−C bond to form enzyme-bound cob(II)alamin and the deoxyadenosyl radical that is kinetically coupled to the next step in the reaction (Scheme 1). The effect of substrate concentration on k_{obs}, the rate of decay of AdoCbl, was used to deconvolute k_f and k_r by use of eq 2. The temperature dependencies of k_f and K_d were analyzed to obtain the thermodynamic activation parameters for Co−C bond homolysis and substrate association steps, respectively.

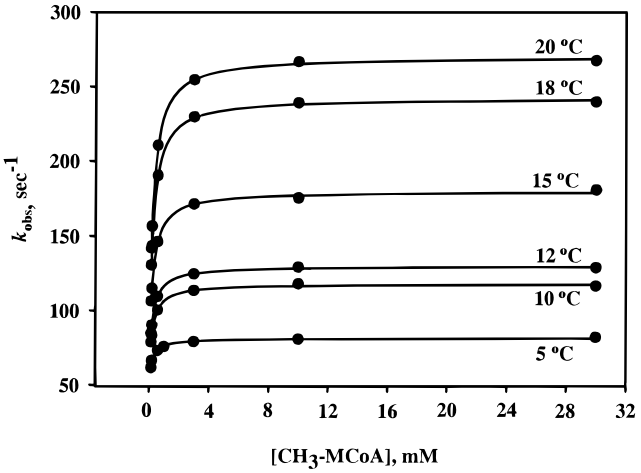

FIGURE 2: Substrate dependence of k_{obs} as a function of temperature. k_{obs} values interpolated from the analysis represented in Figure 1 (inset) were plotted against [CH_3]-methylmalonyl-CoA concentration at six different temperatures. Nonlinear least-squares fit to eq 2 provided k_f, k_r, and K_d (Table 1).

Effect of Methylmalonyl-CoA Concentration on the Rate of Cob(II)alamin Formation. Values for k_f, k_r, and K_d (Table 1) were obtained from nonlinear least-squares fits for the plot of k_{obs} versus substrate concentration (Figure 2) to eq 2. The error in the value of K_d is relatively large (up to 35%), particularly at low temperatures. This is because of the technical limitations in accurately determining the rate of cob(II)alamin formation at low substrate concentration since low enzyme concentrations were also necessary to maintain pseudo-first-order conditions. The K_d for methylmalonyl-CoA binding obtained from this analysis (121 ± 7 μM at 20 °C) is similar to the K_m for CH_3-methylmalonyl-CoA (133 ± 37 μM) (*25*).

Activation Parameters for Substrate Binding and Cob(II)alamin Formation from k_{obs} Data. The values of k_f at different temperatures were plotted in an Eyring plot (Figure 3) to obtain the thermodynamic activation parameters $\Delta H_f^{\ddagger}$ and $\Delta S_f^{\ddagger}$ for cob(II)alamin formation (Table 3). The enthalpy of activation for the formation of cob(II)alamin, $\Delta H_f^{\ddagger}$, is 18.8 ± 0.8 kcal/mol and the entropy of activation, $\Delta S_f^{\ddagger}$, is 18.2 ± 0.8 cal/(mol·K) and corresponds to a $\Delta G_f^{\ddagger}$ of 13.1 ± 0.6 kcal/mol at 37 °C. The lower activation enthalpy for the catalyzed versus the uncatalyzed reaction [34.5 ± 0.8 kcal/mol (*7*)] indicates a positive enthalpic contribution ($\Delta\Delta H^{\ddagger} = 15.7$ kcal/mol) to the lowering of the energy barrier. Similarly, the increase in the activation entropy for the catalyzed versus uncatalyzed reaction [14 ± 1 cal/(mol·K) (*7*)] indicates a small but favorable entropic contribution [$\Delta\Delta S^{\ddagger} = 4.2$ cal/(mol·K)] to the enzyme-catalyzed reaction.

The temperature dependence of K_1 was used in a van't Hoff plot (Figure 4) to determine the enthalpic (ΔH_1) and entropic (ΔS_1) changes associated with substrate binding (Table 3). The value for ΔG_1 is −5.2 ± 0.3 kcal/mol at 37

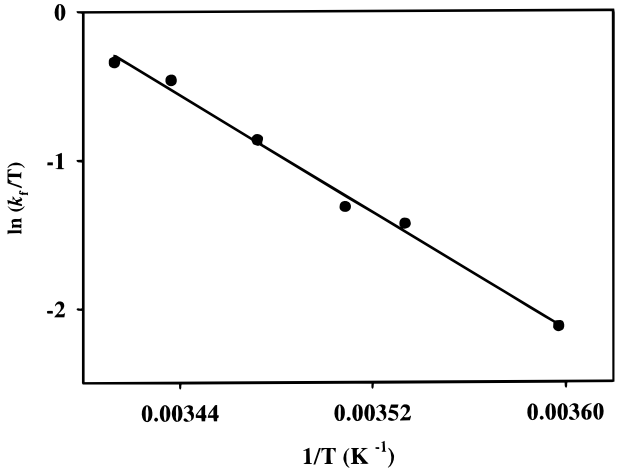

FIGURE 3: Eyring plot for k_f. Values of k_f obtained from the analysis in Figure 2 were plotted as a function of temperature according to the Eyring equation. A linear least-squares fit is shown. The enthalpy and the entropy of activation are obtained from the slope and intercept, respectively, of the best-fit line.

Table 3: Summary of Thermodynamic Parameters

	a	*b*
ΔG_1[c]	-5.2 ± 0.3	-5.2 ± 0.2
$\Delta G_f^{\ddagger}$	13.1 ± 0.6	
ΔH_1[d]	-2 ± 0.1	-2.5 ± 0.1
$\Delta H_f^{\ddagger}$	18.8 ± 0.8	
ΔS_1[e]	10.2 ± 0.5	8.5 ± 0.4
$\Delta S_f^{\ddagger}$	18.2 ± 0.8	

[a] Values in this column were calculated from substrate dependence of k_{obs}. [b] Values in this column were calculated from substrate dependence of v. [c] All ΔG values are in kilocalories per mole at 37 °C. [d] All ΔH values are in kilocalories per mole. [e] All ΔS values are in calories per mole per Kelvin.

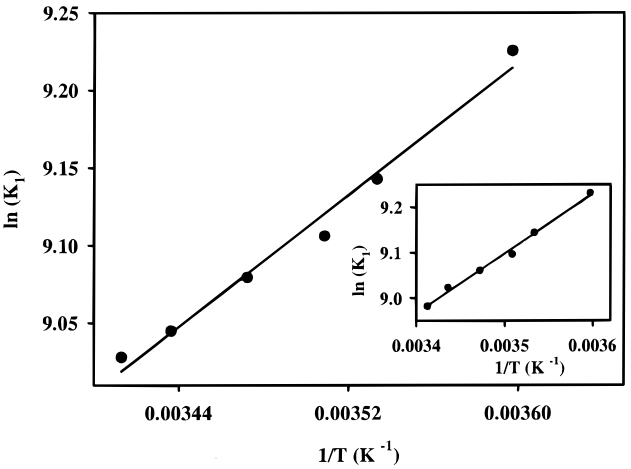

FIGURE 4: van't Hoff plot for K_1. Linear least-squares fit of K_1 (obtained from decay rates in Figure 2) to eq 4 gives ΔH_1 and ΔS_1 from the slope and intercept, respectively. (Inset) Plot of K_1 values (obtained from ν, the fraction of cob(II)alamin at equilibrium) fit to eq 4.

°C. Thus, the substrate binding step is favored by both enthalpic and entropic factors.

Dependence of the Amount of Cob(II)alamin Formed on Methylmalonyl-CoA Concentration. From the amplitude of the absorbance change at 525 nm the equilibrium concentration of cob(II)alamin can be determined. For the mechanism described in Scheme 1, when substrate is in large excess over enzyme, the fraction (ν) of enzyme containing cob(II)-alamin is given by eq 5. A plot of ν versus methylmalonyl-CoA (Figure 5) analyzed by nonlinear least-squares fit to eq 5 gives independent values for K_d (Table 2). At 20 °C, the K_d for the substrate is 125 ± 15 μM. The dissociation constant obtained by this method is similar to that obtained from the kinetic analysis of cob(II)alamin formation (120 ± 7 μM).

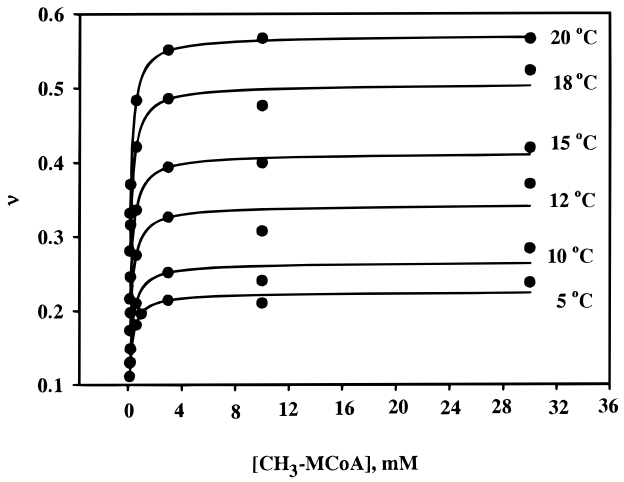

FIGURE 5: Substrate ([CH_3]-methylmalonyl-CoA) dependence of ν (the fraction of total enzyme in the cob(II)alamin state at equilibrium) as a function of temperature. The plots were fit by nonlinear least-squares to eq 5 to obtain K_d and K_2'.

Temperature Dependence of the Amount of Cob(II)alamin Formed. The values of K_1 obtained at each temperature from eq 5 were plotted in a van't Hoff plot (Figure 4, inset) to obtain the thermodynamic parameters (Table 3) for the substrate binding step. This provided an independent check on the thermodynamic parameters obtained from the kinetic data. The relative free energy change, ΔG_1 (-5.2 ± 0.2 kcal/mol at 37 °C), is in excellent agreement with that obtained from the kinetic experiments (-5.2 ± 0.3 kcal/mol).

DISCUSSION

A spectacular aspect of AdoCbl-dependent enzyme-catalyzed reactions is the prodigious enhancement of the Co−C bond homolysis rate that is achieved during catalytic turnover. The bond dissociation energy for base-on AdoCbl in solution is 30 ± 2 kcal/mol (*7*) and the homolysis rate for the uncatalyzed reaction is 3.8×10^{-9} s^{-1} at 37 °C (calculated from the $\Delta H_{hom}^{\ddagger}$ and $\Delta S_{hom}^{\ddagger}$ values in ref *7*). On the basis of the values of $\Delta H_f^{\ddagger}$ and $\Delta S_f^{\ddagger}$ in Table 3, the value for k_f at 37 °C is estimated to be 3339 s^{-1}. The specific rate enhancement achieved by the mutase in the presence of methylmalonyl-CoA is therefore 0.9×10^{12}-fold and corresponds to a $\Delta\Delta G^{\ddagger}$ for cob(II)alamin formation of 16.9 kcal/mol.

One of the hypotheses for explaining the rate acceleration that has been experimentally explored by numerous model studies invokes enzyme-induced ground-state distortion leading to an upward flexing of the corrin ring, causing the Co−C bond to weaken (*9*−*12*). However, resonance Raman studies in which the frequencies of the Co−C stretching vibration have been compared for the free and mutase-bound AdoCbl, demonstrate a very minor destabilization of the Co−C bond corresponding to ~0.5 kcal/mol (*16*−*18*). Thus, the major weakening of the Co−C bond in methylmalonyl-CoA mutase

must be achieved following substrate binding. Both kinetic (*3*) and structural (*26*) evidence support this conclusion. In addition, an EPR signal is not observed for the mutase in the absence of substrate, consistent with substrate-dependent homolysis of the Co−C bond (*27*).

Pre-steady-state analysis of the mutase-catalyzed reaction provided a k_{obs} for homolysis of >600 s^{-1} at 25 °C in the presence of protiated substrate (*3*). This rate slowed to 28 s^{-1} at 25 °C in the presence of [CD_3]-methylmalonyl-CoA, revealing a very large kinetic isotope effect on cleavage of the Co−C bond upon deuterium substitution in the substrate. These results were interpreted as evidence for kinetic coupling of the cleavage of the Co−C bond to the formation of the substrate radical (Scheme 1). This study confirmed that Co−C bond homolysis is triggered by substrate binding and indicated that the intrinsic substrate binding energy may be a significant contributor to the catalytic prowess of methylmalonyl-CoA mutase.

Comparison of the structures of methylmalonyl-CoA mutase in the presence and absence of substrate provides interesting insights into how the substrate may labilize the organometallic bond (*26*, *28*). Binding of methylmalonyl-CoA results in a significant conformational change in a TIM barrel that closes up along the substrate axis. This is accompanied by repositioning of Tyr89 in the active site, which moves closer to the cobalamin, thereby occluding the binding site for the adenosyl moiety. The structures therefore suggest that movement of Tyr89 upon substrate binding may be physically involved in translating some of the substrate binding energy into catalytic power. The conservative mutation of Tyr89 to phenylalanine resulted in a decreased catalytic rate and significantly altered energetics for radical interconversion without affecting K_m (*29*). These results indicate that hydrogen bonding to Tyr89 also plays a role in the rearrangement reaction by differentially stabilizing one or more transition states between the product and substrate radicals.

To quantitatively assess how the enzyme enhances the efficiency of cob(II)alamin formation, we have investigated the thermodynamic parameters associated with this step in the methylmalonyl-CoA mutase reaction. Although the overall reaction catalyzed by methylmalonyl-CoA mutase is linearly dependent on temperature between 5 and 37 °C, the observed rate of homolysis with protiated methymalonyl-CoA is very fast at ambient temperature (>600 s^{-1} at 25 °C). This limits our ability to make accurate measurements by stopped-flow spectrophotometry in a wide temperature range. We have therefore examined the temperature dependence of cob(II)alamin formation between 5 and 20 °C.

These studies have allowed us to construct for the first time a free energy profile for the methylmalonyl-CoA mutase reaction leading up to cob(II)alamin formation (Chart 1). The observed rate of cob(II)alamin formation and the amplitude of the absorption decay of enzyme-bound AdoCbl were employed to obtain independent estimates for K_d, the dissociation constant for the holoenzyme•[CH_3]-methylmalonyl-CoA Michaelis−Menten complex. The values for K_d at 20 °C, 120 ± 7 μM (from k_{obs}, Table 1) and 125 ± 15 μM (from the amplitude change, Table 2), are similar to each other and to the K_m for protiated methylmalonyl-CoA [133 ± 37 μM (*25*)], indicating that the K_d and K_m for methylmalonyl-CoA are the same within experimental error. Binding of substrate is exergonic and is associated with a negative free energy change, $\Delta G_1 = -5.2$ kcal/mol (Table 3).

Chart 1[a]

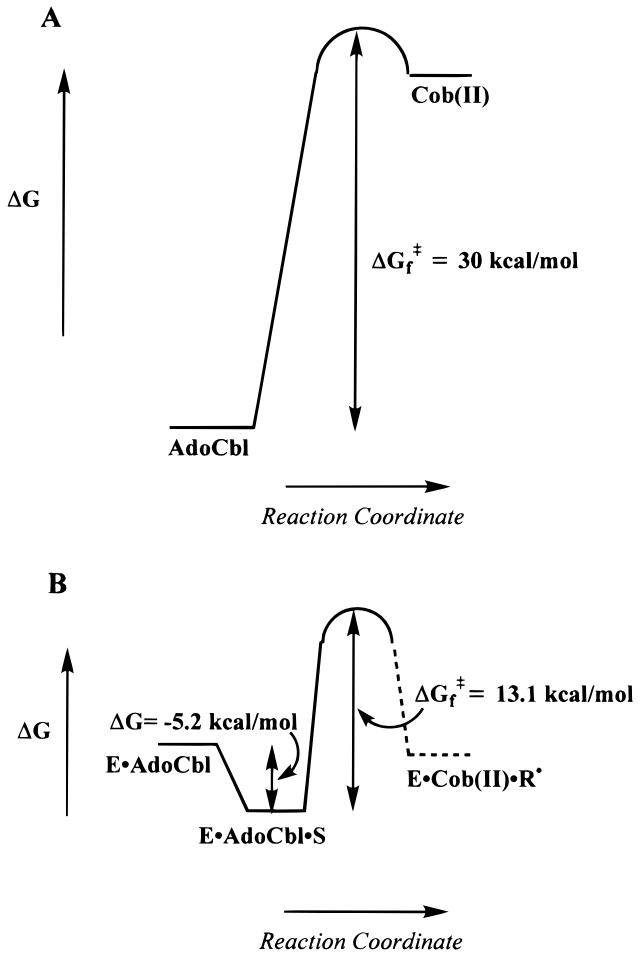

[a] Reaction coordinates for the uncatalyzed (A) and mutase-catalyzed (B) homolysis of the Co−C bond. R• represents an organic radical that could be cofactor-, substrate-, or product-derived. The dashed line represents the hypothetical energy level of the product state.

Weakening of the Co−C bond following binding of substrate needs to be achieved by a combination of transition-state and product stabilization. This is due to the fact that the ΔH for the uncatalyzed homolysis is 30 kcal/mol, and the ΔG for the reaction is estimated to be ~26 kcal/mol (*24*). Thus an upper limit for $\Delta\Delta G_f^‡$ resulting solely from transition-state stabilization is 4 kcal/mol. This is significantly smaller than the value of 16.9 kcal/mol calculated from the ratio of the catalyzed to uncatalyzed homolysis rate constants. Hence, the enzyme-catalyzed reaction is expected to display notably altered energetics compared to the uncatalyzed reaction (Chart 1). Our data reveal a lowering of the Gibbs free energy of activation of the expected magnitude for methylmalonyl-CoA mutase-catalyzed cob(II)alamin formation. Since only the formation of cob(II)alamin is monitored in this study, our kinetic data do not allow distinction between the Ado•, S•, and P• radical states that are each transiently formed along the reaction coordinate while the second radical is located on the cobalt. Furthermore, they do not allow deconvolution of the microscopic rate constant for the reverse rate of AdoCbl formation from cob(II)alamin. Thus, the extent to which the mutase alters the equilibrium

Table 4: Comparison of the Thermodynamic Parameters for AdoCbl Homolysis for Uncatalyzed, Methylmalonyl-CoA Mutase- and Ribonuleotide Reductase-Catalyzed Reactions

	uncatalyzed[a]	methylmalonyl-CoA mutase	ribonucleotide reductase[b]
$\Delta G_f^{\ddagger}$ (kcal/mol at 37 °C)	30.2	13.1 ± 0.6	15.7 ± 0.1
$\Delta H_f^{\ddagger}$ (kcal/mol)	34.5 ± 0.8	18.8 ± 0.8	46 ± 7
$\Delta S_f^{\ddagger}$ [cal/(mol·K)]	14 ± 1	18.2 ± 0.8	96 ± 12

[a] These values were obtained from ref 6. [b] These values were obtained from ref *24*.

between AdoCbl and cob(II)alamin cannot be presently determined.

A comparison of the thermodynamic parameters for the uncatalyzed versus catalyzed Co−C bond homolysis reactions needs to considered with the caveat that in the mutase-catalyzed reaction the homolysis step is kinetically coupled to the subsequent hydrogen atom abstraction step. The methylmalonyl-CoA mutase-catalyzed homolysis reaction is characterized by a substantial lowering of the activation energy barrier ($\Delta G_f^{\ddagger}$ = 13.1 ± 0.6 kcal/mol) for cob(II)-alamin formation, which corresponds to a $\Delta\Delta G^{\ddagger}$ of 17 kcal/mol, coincident with the expectation from the ratio of the catalyzed to uncatalyzed homolysis rate constants. Examination of the $\Delta H_f^{\ddagger}$ and $\Delta S_f^{\ddagger}$ reveals that both enthalpic and entropic factors contribute to rendering the enzyme-catalyzed homolysis reaction favorable. Thus, the activation enthalpy decreases from 34.5 ± 0.8 to 18.8 ± 0.8 kcal/mol, while the activation entropy shows a modest increase from 14 ± 1 to 18.2 ± 0.8 cal/(mol·K) for the enzymatic reaction (Table 4).

It is interesting to compare the energetics of the Co−C bond homolysis reaction catalyzed by methylmalonyl-CoA mutase with that of ribonucleotide triphosphate reductase (Table 4). In the latter enzyme, occupancy of the allosteric effector site is sufficient to cause homolysis of AdoCbl in the absence of substrate, although at a lower rate than under turnover conditions (*24*, *30*). There are two reports in the literature on the thermodynamic parameters associated with the reductase-catalyzed cleavage of AdoCbl (*24*, *31*). Our studies were conducted under pseudo-first-order conditions similar to the work from Stubbe's laboratory, and therefore only these results are discussed here. As in the methylmalonyl-CoA mutase-catalyzed reaction, homolysis is coupled to the next step in the reaction, which is generation of a protein-based thiyl radical in the reductase (*5*). A comparison of the thermodynamic parameters of the uncatalyzed and mutase- and reductase-catalyzed reactions is presented in Table 4. Interestingly, both enzyme-catalyzed reactions stabilize the transition state to a similar extent, causing a lowering in the activation barrier by 16−17 kcal/mol at 37 °C. The difference between the two reactions is that while the mutase-catalyzed reaction is largely enthalpically driven, the reductase reaction is entropically driven. This is most likely due to the differences in the reactions that have been studied in the two cases. The reductase binds AdoCbl rather poorly in contrast to the mutase, where the cofactor is tightly bound, and the kinetic scheme describing homolysis contains a cofactor binding step that is difficult to saturate for the reductase. In contrast, Co−C bond homolysis of tightly bound AdoCbl is triggered by substrate binding to methylmalonyl-CoA mutase, which is readily saturable. Second, the activation parameters for the reductase reaction describe the homolysis step in the absence of substrate and lead to the formation of a protein-based sulfur radical. This is in contrast to the mutase, where the homolysis reaction is only detectable in the presence of substrate and leads to an organic radical.

A complete description of the free energy profile of the methylmalonyl-CoA mutase-catalyzed rearrangement reaction must await a detailed kinetic investigation and identification of key intermediates along the reaction coordinate. In this study, we have characterized the thermodynamic parameters associated only with the substrate binding and cob(II)alamin formation steps. In Chart 2 a qualitative free energy profile for the methylmalonyl-CoA mutase-catalyzed reaction is constructed that incorporates the available information from kinetic (*3*, *29*, *32*) and EPR spectroscopic studies (*21*). Substrate binding is exothermic and is followed by the Co−C bond homolysis step. The immediate products of this reaction are cob(II)alamin and the deoxydenosine radical. The latter has not been detected directly by EPR spectroscopy in any AdoCbl-dependent enzyme. Stopped-flow data from our laboratory have revealed that the homolysis step is kinetically coupled to hydrogen atom abstraction from the substrate (*3*). The deoxyadenosyl and substrate radicals are both primary radicals and are expected to be of approximately equal energy in solution. We have depicted the substrate radical to be slightly lower in energy in Chart 2 since its existence under steady-state conditions is predicted by kinetic studies (*32*) and supported by EPR spectroscopy (*21*; also discussed below). The substrate radical then rearranges to a more stable, secondary, product-centered radical. Tritium partitioning from the 5′ position of AdoCbl into substrate and product, respectively, reveals that under initial velocity conditions the isotope partitions 3:1 in favor of succinyl-CoA regardless of whether the reaction is initiated with substrate or product (*32*). This indicates that the barrier to the interconversion of substrate and product radicals is low and that it does not limit the overall rate (*32*). EPR spectroscopic studies provide evidence for the existence of two organic radicals coupled to cob(II)alamin. These have distinct power saturation properties and could represent a mixture of substrate- and product-derived radicals at slightly different distances from the metal radical (*21*). Reabstraction of a hydrogen atom from deoxydenosine by the product radical regenerates the primary deoxyadenosyl radical that recombines with cob(II)alamin to complete the reaction.

The overall equilibrium for the rearrangement reaction favors succinyl-CoA formation by a factor of 23 (*33*). The two hydrogen transfer steps, i.e., from substrate to the deoxyadenosyl radical and from deoxyadenosine to the product radical, are expected to be isotope-sensitive. An anomalously large primary deuterium isotope effect [∼36 at 20 °C (*34*)] is associated with hydrogen atom transfer from the substrate (*3*). However, the overall deuterium isotope effect on V_{max} with [CD_3]-methylmalonyl-CoA is 6.2 (*35*). Thus, suppression of the intrinsic deuterium isotope effects during steady-state turnover must result from an isotopically insensitive step that limits the rate of catalytic turnover.

Under steady-state conditions, the ratio of cob(II)alamin to AdoCbl is approximately 1:4, consistent with a step following AdoCbl re-formation being rate-limiting (*3*). On

Chart 2[a]

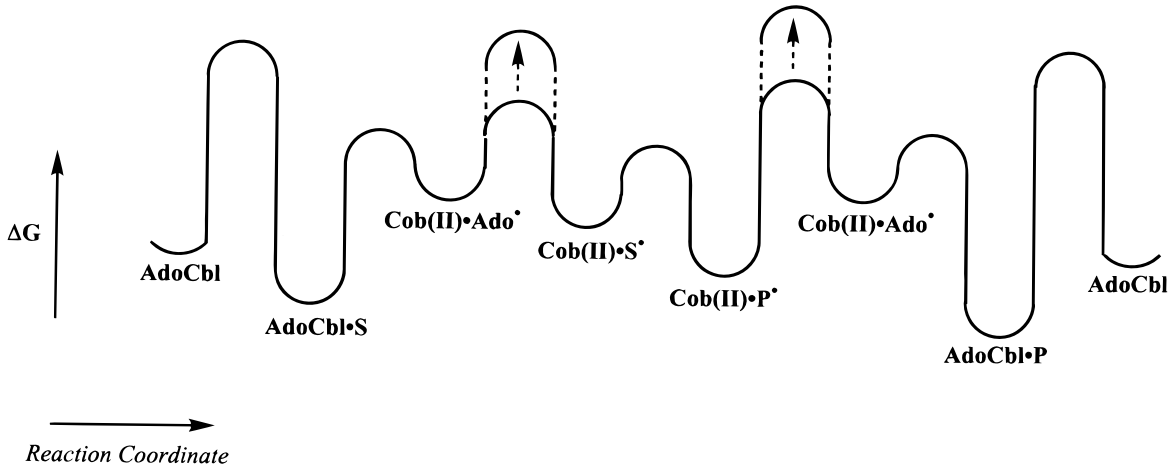

[a] Qualitative free energy profile for the methylmalonyl-CoA mutase reaction. Ado•, S•, and P• represent the deoxyadenosine, substrate, and product radicals, respectively. The dashed arrows indicate the hydrogen transfer steps that are isotope-sensitive.

the basis of the available data, we predict that the radical pair intermediates that have been visualized by EPR spectroscopy represent a mixture of the substrate and product radicals [in a ratio of 1:3 (32)] coupled to cob(II)alamin and that the major bottleneck in the reaction occurs at the product release step, leading to the predominance of AdoCbl under steady-state conditions (*3*).

The issue of kinetic versus chemical coupling of the homolytic cleavage and hydrogen transfer steps cannot be addressed by these studies, which examine the temperature dependence of the rate of cob(II)alamin formation at different substrate concentrations. Kinetic coupling of the two steps can occur via either stepwise or concerted mechanisms. The geometric constraints required for a concerted reaction are rather stringent and are less likely to be met for *both* the forward and reverse reactions in the enzyme active site. Thus, while these studies do not address the issue of chemical coupling, the more likely stepwise mechanism has been depicted in Scheme 1 and Chart 2.

Qualitative free energy profiles for two other AdoCbl-dependent isomerases have been reported recently (*36*, *37*). In glutamate mutase, which also catalyzes a carbon skeleton rearrangement reaction, the predominant radical that is observed under steady-state turnover conditions is the substrate C4 glutamyl radical (*38*). Rearrangement of the substrate radical is postulated to be rate−limiting in this reaction (*36*). In contrast, the product radical is observed under steady-state conditions with ethanolamine ammonia lyase, and reabstraction of a hydrogen atom from deoxyadenosine is postulated to be rate-determining (*37*). In glutamate mutase, as in methylmalonyl-CoA mutase, the intrinsic deuterium isotope effect is suppressed. The deuterium isotope effects for the overall reaction and for hydrogen transfer from substrate are 3.9 (*39*) and 28 (*4*), respectively, in glutamate mutase. Thus, in both these enzymes, hydrogen transfer steps that are characterized by anomalously large isotope effects are not fully rate-determining, although the slowest step in these reactions have yet to be unambiguously identified and appear likely to be different. Under steady-state conditions, AdoCbl is the predominant cofactor form in methylmalonyl-CoA mutase (*3*) and in glutamate mutase (*4*). This also appears to be the case with ethanolamine ammonia lyase, where the spins associated with the organic radical intermediate represent only 20% of the total for the enzyme (*37*).

In summary, we report the thermodynamic parameters associated with substrate-induced Co−C bond cleavage in methylmalonyl-CoA mutase. Our studies provide a description of the free energy profile of methylmalonyl-CoA mutase through the substrate-induced homolysis step and provide insights into how the large rate enhancement is achieved. The enzyme lowers the transition-state barrier by 17 kcal/mol at 37 °C. Both entropic and enthalpic factors contribute to the rate acceleration in methylmalonyl-CoA mutase with the latter predominating.

REFERENCES

1. Banerjee, R. (1997) *Chem. Biol. 4*, 175−186.
2. Banerjee, R., and Chowdhury, S. (1999) in *Chemistry & Biochemistry of B_{12}*, (Banerjee, R., Ed.) pp 707−730, John Wiley and Sons, New York.
3. Padmakumar, R., Padmakumar, R., and Banerjee, R. (1997) *Biochemistry 36*, 3713−3718.
4. Marsh, E. N. G., and Ballou, D. P. (1998) *Biochemistry 37*, 11864−11872.
5. Licht, S. S., Booker, S., and Stubbe, J. (1999) *Biochemistry 38*, 1221−1233.
6. Finke, R. G., and Hay, B. P. (1984) *Inorg. Chem. 23*, 3041−3043.
7. Waddington, M. D., and Finke, R. G. (1993) *J. Am. Chem. Soc. 115*, 4629−4640.
8. Hay, B. P., and Finke, R. G. (1987) *J. Am. Chem. Soc. 109*, 8012−8018.
9. Grate, J. H., and Schrauzer, G. N. (1979) *J. Am. Chem. Soc. 101*, 4601−4611.
10. Marzilli, L. G., Toscano, J., Randaccio, L., Bresciani-Pahor, N., and Calligaris, M. (1979) *J. Am. Chem. Soc. 101*, 6754−6756.
11. Glusker, J. P. (1982) in *B12* (Dolphin, D., Ed.) Vol. 1, pp 23−106, Wiley, New York.
12. Brown, K. L., and Brooks, H. B. (1991) *Inorg. Chem. 30*, 3420−3430.
13. Kräutler, B., Konrat, R., Stupperich, E., Gerald, F., Gruber, K., and Kratky, C. (1994) *Inorg. Chem. 33*, 4128−4139.
14. Ng, F. T. T., Rempel, G. L., and Halpern, J. (1982) *J. Am. Chem. Soc. 104*, 621−623.
15. Geno, M. K., and Halpern, J. (1987) *J. Am. Chem. Soc. 109*, 1238−1240.

16. Dong, S., Padmakumar, R., Banerjee, R., and Spiro, T. G. (1996) *J. Am. Chem. Soc. 118*, 9182−9183.
17. Dong, S., Padmakumar, R., Banerjee, R., and Spiro, T. G. (1998) *Inorg. Chim. Acta 270*, 392−398.
18. Dong, S., Padmakumar, R., Maiti, N., Banerjee, R., and Spiro, T. G. (1998) *J. Am. Chem. Soc. 120*, 9947−9948.
19. Dong, S., Padmakumar, R., Banerjee, R., and Spiro, T. G. (1999) *J. Am. Chem. Soc. 121*, 7063−7070.
20. McKie, N., Keep, N. H., Patchett, M. L., and Leadlay, P. F. (1990) *Biochem. J. 269*, 293−298.
21. Padmakumar, R., and Banerjee, R. (1995) *J. Biol. Chem. 270*, 9295−9300.
22. Taoka, S., Padmakumar, R., Lai, M.-t., Liu, H.-w., and Banerjee, R. (1994) *J. Biol. Chem. 269*, 31630−31634.
23. Licht, S., Gerfen, G. J., and Stubbe, J. (1996) *Science 271*, 477−481.
24. Licht, S. S., Lawrence, C. C., and Stubbe, J. (1999) *Biochemistry 38*, 1234−42.
25. Maiti, N., Widjaja, L., and Banerjee, R. (1999) *J. Biol. Chem. 274*, 32733−32737.
26. Mancia, F., and Evans, P. (1998) *Structure 6*, 711−720.
27. Zhao, Y., Such, P., and Retey, J. (1992) *Angew. Chem., Int. Ed. Engl. 31*, 215−216.
28. Mancia, F., Smith, G. A., and Evans, P. R. (1999) *Biochemistry 38*, 7999−8005.
29. Thomä, N. H., Meier, T. W., Evans, P. R., and Leadlay, P. F. (1998) *Biochemistry 37*, 14386−14393.
30. Orme-Johnson, W. H., Beinert, H., and Blakley, R. L. (1974) *J. Biol. Chem. 249*, 2338−2343.
31. Brown, K. L., and Li, J. (1998) *J. Am. Chem. Soc. 120*, 9466−9474.
32. Meier, T. W., Thomä, N. H., and Leadlay, P. F. (1996) *Biochemistry 35*, 11791−11796.
33. Kellermeyer, R. W., Allen, S. H. G., Stjernholm, R., and Wood, H. G. (1964) *J. Biol. Chem. 239*, 2562−2569.
34. Chowdhury, S., and Banerjee, R. (2000) *J. Am. Chem. Soc. 122*, 5417−5418.
35. Michenfelder, M., Hull, W. E., and Retey, J. (1987) *Eur. J. Biochem. 168*, 659−667.
36. Chih, H. W., and Marsh, E. N. (1999) *Biochemistry 38*, 13684−91.
37. Warncke, K., Schmidt, J. C., and Ke, S.-C., (1999) *J. Am. Chem. Soc. 121*, 10522−10528.
38. Bothe, H., Darley, D. J., Albracht, S. P., Gerfen, G. J., Golding, B. T., and Buckel, W. (1998) *Biochemistry 37*, 4105−13.
39. Chen, H. P., and Marsh, E. N. (1997) *Biochemistry 36*, 14939−45.

BI992535E